Structural and electronic properties of the liquid polyvalent elements. IV. The pentavalent semimetals and trends across the periodic table

J. Hafner and W. Jank
Institut für Theoretische Physik, Technische Universität Wien, Wiedner Hauptstrasse 8-10, A-1040 Wien, Austria
(Received 12 June 1991; revised manuscript received 24 September 1991)

We present *ab initio* calculations of the atomic structure, the electronic density of states, and the photoemission intensities of the molten pentavalent semimetals As, Sb, and Bi. The investigations are based on pseudopotential-based interatomic forces, molecular-dynamics simulations for the liquid structure, and self-consistent linear-muffin-tin-orbital calculations of the electronic structure and photoemission intensities. We show that the anomalous structures of liquid As, Sb, and Bi arise from the modulation of the random packing of atoms by the Friedel oscillations in the effective interatomic potential. These modulations are damped by relativistic effects, which also lead to the formation of an *s-p* gap in the electronic density of states. The position and width of the gap are also shown to be related to the liquid structure. Trends in the atomic and electronic structures of the polyvalent elements across the Periodic Table are discussed.

I. INTRODUCTION

In a recent series of papers[1,2] we have presented a systematic investigation of the trends in the structural and electronic properties of the liquid *s-p*–bonded elements. We have been able to show that the formation of open, low-coordinated structures in the light polyvalent elements (Ga,Si,Ge) arise from the modulation of the random packing of atoms by the Friedel oscillations in the effective interatomic potentials. For the heavy elements we have demonstrated that relativistic effects lead to a damping of the Friedel oscillations, to a return to more closely packed liquid structures, and to the formation of a characteristic "*s-p* dehybridization gap" in the electronic spectrum.

The present work extends these investigations to the semimetals As, Sb, and Bi. These elements crystallize in the trigonal $A7$ structure,[3] which may be regarded as a distorted simple-cubic structure produced by an elongation along one of the [111] directions. This leads to the formation of puckered layers containing six-membered rings of atoms. The mechanism driving the distortion is a Peierls instability of the half-filled p band in the simple-cubic structure.[4,5] The coordination within the layers is three, in accordance with the Hume-Rothery "8-N" rule. This rule states that covalent bonding in compounds with an average of N valence electrons requires 8-N neighbors. Despite the largely covalent character of the bond, the elements are semimetallic[6] because the bonding and antibonding ($pp\sigma$) bands show a small overlap. From As to Bi there is a tendency to equalize the short intralayer and the long interlayer bonds (their ratio drops from 1.25 in As to 1.17 in Sb and 1.12 in Bi), and to reduce the deviation of the bond angle between the short bonds from 90° (the bond angles are 97° in As and 95.5° in Sb and Bi). In the electronic spectrum this is reflected in a larger band overlap and a narrowing of the pseudogap.[7]

The liquid structure of As is surprisingly close to the structure of the crystal: nearest-neighbor bond length, coordination number, and bond angle are hardly affected by melting.[8] On melting As behaves like a normal metal—decreasing conductivity—unlike other covalent elements (e.g., Si, Ge, and Te) for which the conductivity increases on melting.[9] The implication is again that As retains at least initially some of the threefold coordination and of the covalent character of the bond on melting. Liquid Sb and Bi are bad metals, with a conductivity that is of the same order as that of most molten transition metals.[10] The liquid structure of Sb and Bi is still anomalous, with pronounced shoulders in the static structure factor and in the pair-correlation functions.[11–15] The coordination number is definitely enhanced on melting, but the experimental values quoted in the literature differ widely, for liquid Sb between $N_c = 4.6$ (Ref. 11) and $N_c = 8.7$ (Ref. 12). The electronic structure of liquid Bi has been investigated by photoemission spectroscopy.[16] It was found that the electronic density of states at the Fermi level is metallic and that the valence band is split into two bands with essentially s- and p-like symmetries. In the crystalline state, a characteristic splitting of both the s- and p-bands is observed, which is attributed to the Peierls distortion of the lattice. This Peierls splitting is absent in the liquid phase.

Various attempts have been made to explain the open structure of liquid As. Gaspard *et al.*[17] have presented qualitative arguments within a tight-binding framework that a Peierls distortion can occur even in the absence of translational symmetry. Hafner[18] has presented a molecular-dynamics calculation based on effective-pair interactions derived from pseudopotential perturbation theory and achieved quantitative agreement with the diffraction data. He demonstrated that the open, low-coordinated structure arises from a modulation of the random packing of atoms by the Friedel oscillations in the pair potentials. He argued that this mechanism provides an explanation for all the low-coordinated liquid structures of the elements in groups IV, V, and VI of the periodic table and constitutes the appropriate real-space

formulation of the Peierls distortion argument.[19,20] Li *et al.*[21] performed an *ab initio* density-functional molecular-dynamics (DF-MD) calculation of the structure of liquid As and largely confirmed the results of the pair-potential molecular-dynamics study.[18] Significant differences are found only at the level of four-body correlations functions. The electronic structure of crystalline As, Sb, and Bi has been thoroughly well investigated. Electronic structure calculations[22–25] are in full agreement with the existing photoemission data[7] and explain[24–26] the pressure-induced phase transitions from the *A*7 to the simple cubic and to the body-centered-cubic structure. The electronic density of states of liquid As was calculated by Hafner and Payne[27] using dynamical simulated annealing on the basis of a structural model created by pair-potential molecular dynamics, and by Li *et al.*[21] using *ab initio* density-functional molecular dynamics. The two results are in good agreement, except in a narrow region at the Fermi level. The formation of a pseudogap is found to be extremely sensitive to multiple-ion correlations. No attempt has been made as yet to extend the theoretical investigations to liquid Sb and Bi.

In the present work we follow the same strategy as in our previous papers: we use pseudopotential-derived interatomic forces and molecular dynamics for the atomic structure and self-consistent linear-muffin-tin-orbital (LMTO) supercell calculations for the electronic density of states and the photoemission intensity. For the technical aspects we refer entirely to Ref. 1. Our results are presented below.

II. INTERATOMIC FORCES AND ATOMIC STRUCTURE

A. Pair interactions

The relation between the variations of the effective interatomic interactions with electron density and pseudopotential and the systematic trends in the crystalline and liquid structures has been clarified by Hafner and Heine[28] and Hafner and Kahl.[29] It was shown that for the light polyvalent metals a large on-Fermi-surface matrix element leads to a large amplitude of the Friedel oscillations in the effective pair interaction, and a large electron density leads to a large repulsive diameter of the pseudoatom formed by the ionic core plus the screening charge distribution. As a result the first attractive minimum in the pair interaction is covered up by the repulsive interaction, and the nearest-neighbor distance in a close-packed structure (which is determined by the interplay of the pair and volume forces[30,31]) falls on a repulsive hump of the pair potential. Hence a distortion of the structure in a way that corresponds largely to a Peierls distortion is energetically favorable. This is the situation discussed in detail in the previous work by one of us on *l*-As (Ref. 18) and *l*-Te (Ref. 19).

For the heavy elements the combined effect of the variation of the atomic size and of an increased nonlocality of the pseudopotential (largely through relativistic effects) leads to a reduction of the on-Fermi-surface matrix element and hence of the amplitude of the Friedel oscillations. For Tl and Pb this leads to an interatomic potential that is entirely of a screened-Coulomb form[1,28] and stabilizes a close-packed arrangement of the atoms in the crystalline as well as in the liquid state. Bi is a borderline case, with a pair interaction that has an extremely small curvature for distances corresponding to the nearest-neighbor shell.

The original study of Hafner and Heine[28] was based on simple local model potentials of the "empty-core" form,[32] the core radius being adjusted so as to follow the trend deduced from band-structure data and to produce the correct trend in the pair interactions. For a quantitative calculation of the liquid structure of the heavy polyvalent metals it turned out that these potentials are not sufficiently accurate:[33] with a simple one-parameter potential it is impossible to reproduce simultaneously the trend in the atomic radii and in the on-Fermi-surface matrix elements. In our work on liquid Hg, Tl, and Pb we found it necessary[1] to use nonlocal pseudopotentials based on an orthogonalized-plane-wave (OPW) expansion of the valence states, carefully optimized for the convergence of the perturbation series.[31,34] For the heavy metals a fully relativistic calculation of the core states is necessary.[1] For nonperturbative total-energy calculations, the optimized OPW pseudopotentials have been largely superceded by norm-conserving pseudopotentials designed such as to provide optimum transferability and plane-wave convergence.[35–37] The convergence of a perturbation expansion of the total energy based on norm-conserving potentials, however, turns out to be bad.[38] This means that the norm-conserving pseudopotentials are not immediately suited for the construction of effective pair interactions. Very recently, we have been able to show that it is possible to optimize both plane-wave convergence and convergence of the perturbation series without compromising transferability.[39] It turns out that the effective pair interactions derived from the optimized norm-conserving pseudopotentials are almost identical to those derived from the optimized OPW pseudopotentials

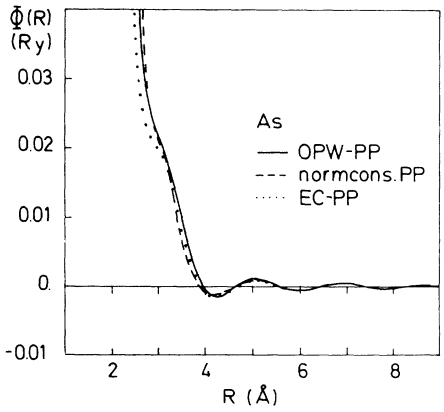

FIG. 1. Effective pair interaction $\Phi(R)$ for liquid As, calculated using the optimized orthogonalized-plane-wave (OPW) pseudopotential (PP) (full line), the optimized norm-conserving potential (dashed line), and the empty-core (EC) model potential used in Ref. 18 (dotted line).

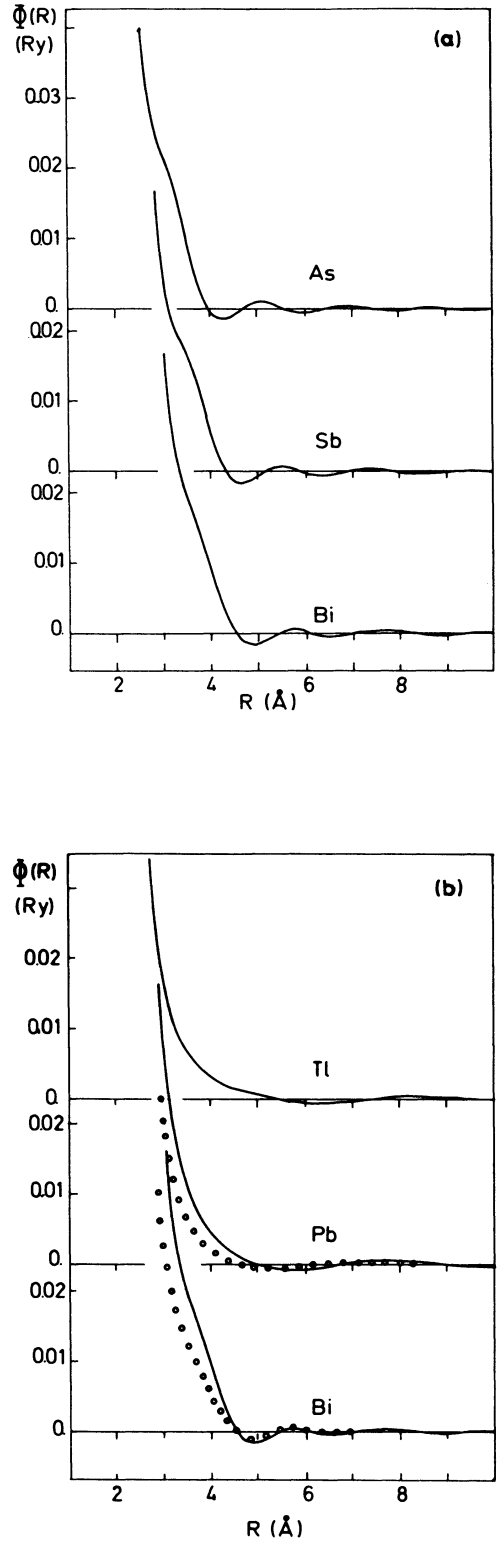

FIG. 2. (a) Effective pair interactions $\Phi(R)$ in liquid As, Sb, and Bi, calculated using the optimized orthogonalized-plane-wave pseudopotentials and a full relativistic treatment of the core states (see text). (b) $\Phi(R)$ in liquid Tl, Pb, and Bi. The full lines give the pseudopotential-derived pair interaction and the dotted lines the result of the inversion of the structure data (after Refs. 14, 39, and 40).

and to those derived from the adjusted model potentials. This holds at least for the lighter elements such as As; see Fig. 1. It shows that quite different approaches to the electron-ion pseudopotential yield a unique answer for the effective pair interaction, if the pseudopotential is optimized for the convergence of the perturbation series (details of the optimization procedure for the norm-conserving potentials will be published elsewhere[39]). For the heavier elements, the local model potential is again found to be insufficient for quantitative calculations, but the trend predicted by Hafner and Heine[28] is fully confirmed by the OPW pseudopotentials with a relativistic core (Fig. 2): the Friedel oscillations are strongly damped, and in liquid Bi the only trace left of the oscillations around the nearest-neighbor distance is a region of nearly zero curvature in $\Phi(R)$. This region of zero curvature represents the characteristic difference between the pair potentials in liquid Bi on one hand and liquid Tl and Pb on the other hand: in the latter elements the curvature is negative throughout [Fig. 2(b)]. This leads to a hard-sphere-like liquid structure for Tl and Pb, but a distinctly anomalous structure factor for Bi (cf. below). It is true that the precise form of the potential is rather sensitive to the form of the exchange-correlation potential. For liquid Bi we found it necessary to reduce the core-valence exchange potential slightly [choosing a constant $\alpha = 0.5$ instead of $\alpha = 2/3$ in Eq. (1) of Ref. 1] in order to avoid the curvature becoming slightly positive. This is in agreement with the general trend, we refer to the discussion in Ref. 1(c).

Over the past 25 years, many attempts have been made to extract empirical potentials from accurate structure data. Nearly all of the early attempts failed, both because of insufficient accuracy of the experimental data and because of instabilities of the inversion procedure. Now, this problem has been solved by improved diffraction data and reliable iterative inversion algorithms.[14,40-42] For liquid Pb and Bi, the empirical pair potentials are in very good agreement with those derived from the pseudopotential perturbation expansion [Fig. 2(b)], the only difference is in a slight shift of the repulsive core.

B. Atomic structure

The atomic structure was calculated using constant-energy molecular dynamics (for technical details see Ref. 1) for ensembles containing between 1000 and 2000 atoms, models for the supercell calculations of the electronic structure were prepared by repeating the simulations for 64-atom ensembles.

Figures 3 and 4 compare the calculated pair-correlation functions and static structure factors with the available diffraction data. Compared to a hard-sphere-like fluid, the second maximum in $g(R)$ is shifted to larger distances (the ratio $R_2/R_1 = 2.28$, 2.00, and 1.93 for As, Sb, and Bi, compared to $R_2/R_1 \approx 1.89$ for a hard-sphere liquid), and a small intermediate maximum is found close to the main peak. The origin of this side peak is clearly related to the form of the pair interaction: the upward curvature of $\Phi(R)$ leads to a Peierls-like splitting of the nearest-

neighbor shell, even for liquid Bi where the curvature is essentially zero at the nearest-neighbor distance. In liquid As the first peak in $g(R)$ contains about three atoms, the second nine (the exact values depend somewhat on the way the coordination number is calculated: from an integral over the radial distribution function up to the first minimum, or from an integral over the symmetric part of the peak).[12] This result is quite independent from the choice of a pseudopotential. In liquid Sb and Bi both the nearest-neighbor and next-nearest-neighbor coordination numbers Z_1 and Z_2 are increased (cf. Table I), their sum approaches the value $Z_1 + Z_2 = 18$ appropriate for a close-packed structure. A similar conclusion may be drawn from the bond-angle distributions (Fig. 5). For liquid As one finds a strong preference for bond angles close to those in either the rhombohedral or orthorhombic crystalline phase of As, and side peaks at bond angles of $\theta \approx 60°$ and 180°. Note that there are only minor quantitative differences between our result and the quantum-mechanical many-body simulation of Li *et al.*[21] The first significant difference appears in a four-body correlation, namely, the distribution of the heights h of the trigonal As_4 pyramids. The distribution is rather diffuse in the pair-potential calculation, where as a distinct peak around $h \approx 1$ Å appears in the many-body simulation (see Ref. 21 for details). In liquid Sb and Bi the 60° peak becomes dominant, and a third peak near $\theta \approx 145°$ has appeared. This third peak arises from the angles formed

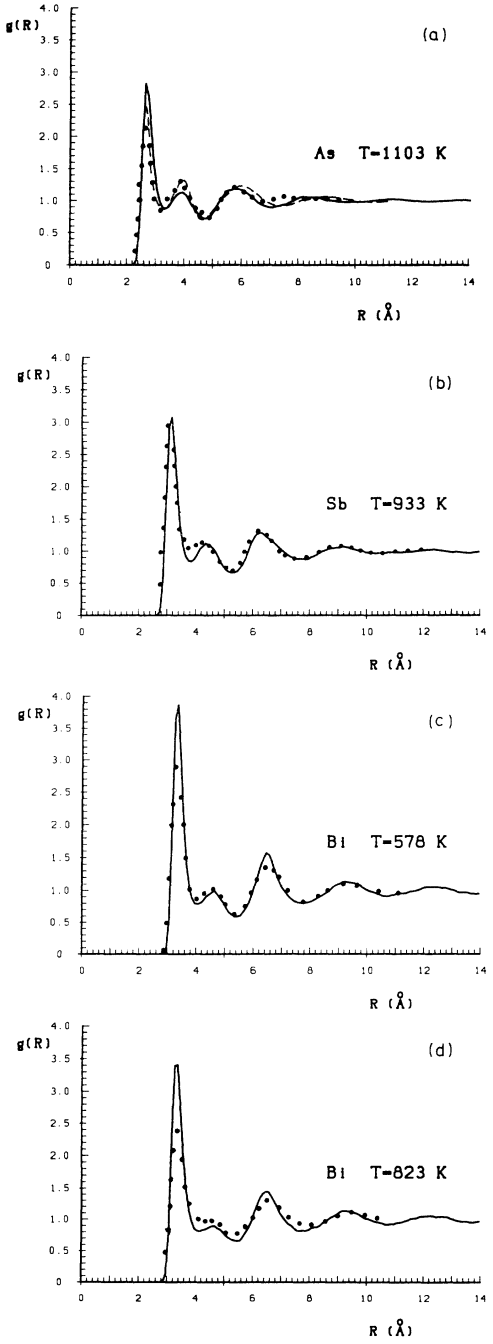

FIG. 3. Pair correlation function $g(R)$ for liquid As (a), Sb (b), and Bi (c) and (d). Full line—molecular-dynamics simulation—OPW-potentials, dashed line—molecular-dynamics simulation—EC potential, dots—diffraction data (As—Ref. 8, Sb—Ref. 11, and Bi—Refs. 13–15).

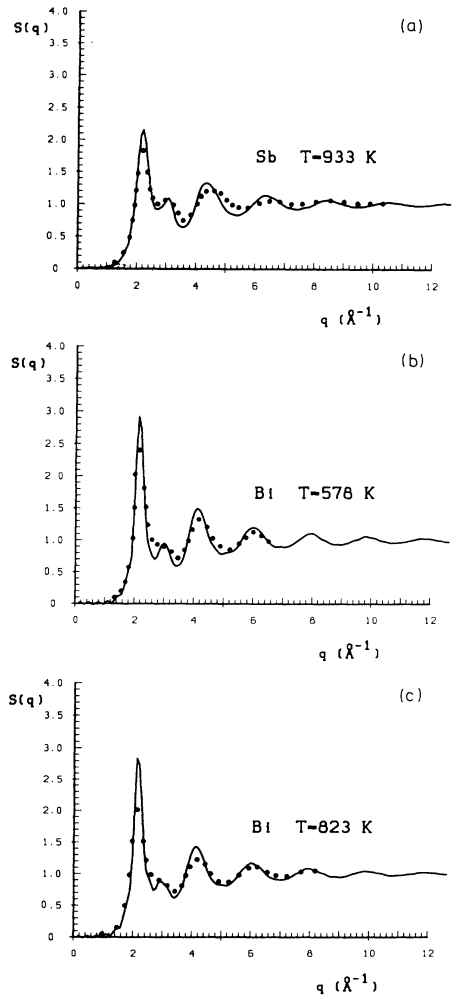

FIG. 4. Static structure factor $S(q)$ for liquid Sb (a) and Bi (b) and (c). Full line—molecular-dynamics simulation, dots—diffraction data (Sb—Ref. 11 and Bi—Refs. 13–15).

TABLE I. Coordination numbers Z_i for the first two coordination shells in liquid As, Sb, and Bi.

	MD simulation		Experiment		
	Z_1 [a]	Z_2 [b]	Z_1	Z_2	Ref.
As	3.0	9.2	3.0	8.9	8
Sb	5.2	10.1	4.6		11
Bi	7.1	10.8	6.7		13

[a] Calculated by integrating over the symmetric part of the first peak in the radial distribution function.

[b] Calulated by integrating the radial distribution function up to the second minimum.

by nearest-neighbor bonds and what would be the back bonds in the crystalline structure. In the heavier elements, the difference between bonds and back bonds is gradually washed out. Note that the bond-angle distribution of Sb and Bi is close to that of As under elevated pressure.[21]

The first peak in the static structure factor is determined by the distance of closest approach, the second peak is determined by the Fermi momentum, $Q_2 \leq 2k_F$ (see Fig. 4). This confirms that the complex structure of the molten semimetals arises from the interplay of two characteristic distances, the diameter of the repulsive core in the potential, and the Friedel wavelength $\lambda_F = 2\pi/2k_F$ of the long-range oscillations.[28,31] The second peak decreases in intensity with increasing atomic number. The molecular dynamics simulation reproduces this result, although the structure of the side peak is much sharper in the simulation than in the diffraction data. This would seem to indicate that the modulation of the structure by the oscillations in the potential is predicted to be of longer range than in reality. However, this is not entirely confirmed by the correlation functions, where the only significant disagreement is in the height of the main peak. This is probably related to the limited Q range of the diffraction data—a termination of the Fourier transform at low q leads to a broadening of the peaks in the correlation function. We also note that there is considerable disagreement between the existing experimental data: older data compiled in the literature[12] generally show much less structure than the more recent data[8,11,13,14] shown in our figures. Altogether we find that our potentials lead to quite accurate liquid structures for As, Sb, and Bi. Even more important, we demonstrate that the open, low-coordinated structures of all polyvalent elements from Ga to Bi have a common origin: the Friedel modulation of the dense random packing or, in other words, a Peierls distortion.

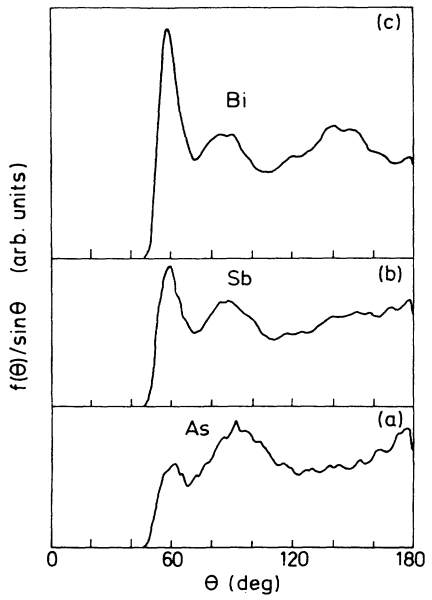

FIG. 5. Bond-angle distribution function $f(\theta/\sin\theta)$ for liquid As, Sb, and Bi. $f(\theta)$ has been normalized the same number of bonds.

III. ELECTRONIC SPECTRUM

In the following we discuss the electronic densities of states calculated using the scalar-relativistic LMTO technique[43,44] for supercells containing representative configurations of the liquid elements and for the stable crystalline structure (data given in Table II). All technical details are given in Ref. 1. The application of the LMTO in the atomic sphere approximation (ASA) (LMTO-ASA) to a low-coordinated structure deserves some comments. In the diamond structure one finds it necessary to put empty spheres into the holes in the lattice (which are as large as the atomic spheres). The $A7$ structure of the pentavalent elements is derived by a Peierls distortion of the simple-cubic structure. The difference between the three short and three long bonds is at most 25% and only 12% in Bi. Therefore, the volume available for empty spheres is much smaller than in the diamond lattice. Comparing the LMTO-ASA result with pseudopotential calculations for the crystalline elements,[24,25] no significant difference is found. The same conclusions result from comparing the present LMTO results for liquid As with the dynamical-simulated-annealing calculations of Hafner and Payne;[27] for details see below.

A. Electronic density of states

The electronic densities of states are given in Figs. 6–8. Both in the crystalline and in the liquid states the valence band is separated in an s band at higher binding energy and a p band at the Fermi level. In As and Sb s and p bands show a very small overlap; in Bi they are separated by a gap of approximately 3 eV. In the crystal, the rhombohedral distortion leads to a symmetric splitting of both the s and p bands. As pointed out by Ley and coworkers[7,45] in their analysis of x-ray photoemission data, the splitting of the s-like peak scales with the nearest-neighbor distance. The density of states (DOS) calculated using the LMTO is in very good agreement with the linearized-augmented-plane-wave result of Mattheiss, Hamann, and Weber[24] and with the pseudopotential results of Needs, Martin, and Nielsen.[25] Mattheiss *et al.*

TABLE II. Number densities of crystalline and liquid As, Sb, and Bi, and intra- and interlayer distances d_1 and d_2 in the rhombohedral phases.

	n (Å)		d_1 (Å)	d_2 (Å)	d_2/d_1
	Liquid	Crystalline			
As	0.0422	0.0465	2.51	3.15	1.25
Sb	0.0321	0.0331	2.87	3.37	1.17
Bi	0.0289	0.02908	3.10	3.47	1.12

have pointed out that the splitting of the s band has only minimal effect on the stability of the rhombohedral phase, whereas the splitting of the p band causes an appreciable lowering of the band energy from the states just below E_F.

The splitting of the s bands disappears if the translational symmetry is broken—this appears very clearly in the valence-band spectra of amorphous As, Sb, and Bi.[45] Greaves and co-workers[9,46] have shown that the bifurcation of the s band is related to the ring structure of the $A7$ lattice: in the crystalline structure there are only regular six-numbered rings, as in the diamond structure. The splitting of the s band corresponds to the splitting of the two lowest peaks in the sp^3-hybridized band of the tetrahedral semiconductors. The disappearance of the bifurcation corresponds to the appearance of odd-numbered rings in a continuous random-network[46] model. On the other hand the splitting of the p band subsists in the amorphous state of all three elements.

In the liquid state both the s and p bands are unsplit. The unoccupied part of the p band is separated by a pseudogap from the d band (Figs. 6–8).

For liquid As we include for comparison the result obtained by Hafner and Payne[27] via a dynamical-simulated-annealing (DSA) calculation using a local pseudopotential and a basis of about 4000 plane waves. The result of the DSA calculation is not as smooth as the DOS resulting from the LMTO calculations. This is due to the fact that only a single **k** point has been used, compared to the complete star of 32 special points used in the LMTO. Apart from this minor difference, both calculations are in good agreement. This shows that, as mentioned above, the LMTO-ASA is adequate for these low-coordinated liquid structures.

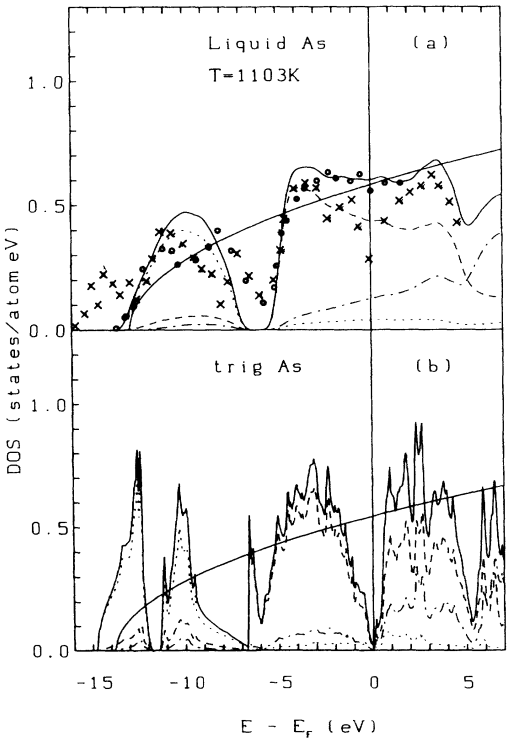

FIG. 6. Electronic density of states for liquid (a) and crystalline (b) As. Solid line—total DOS, dotted line—s, dashed line—p, dot-dashed line—d—electron contribution. The open circles show the results of the dynamical-simulated-annealing (DSA) calculation of Hafner and Payne (Ref. 27); the crosses are the results of the *ab initio* density-functional molecular-dynamics calculation of Li *et al.* (Ref. 21).

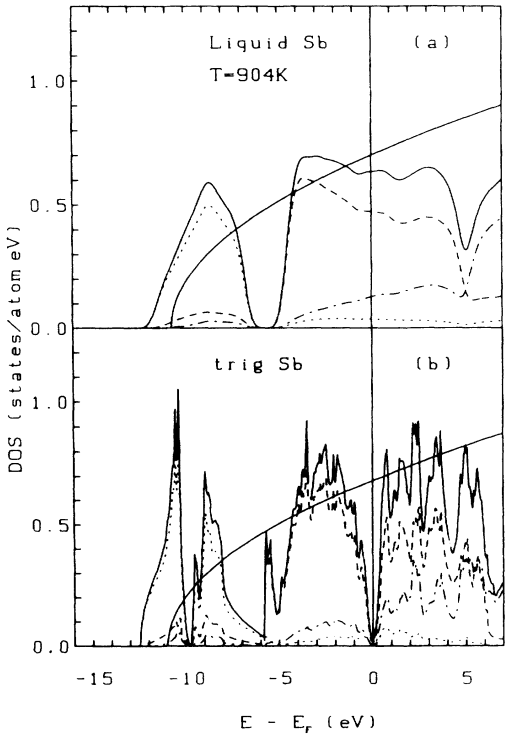

FIG. 7. Electronic density of states for liquid (a) and crystalline (b) Sb. For the key see Fig. 6.

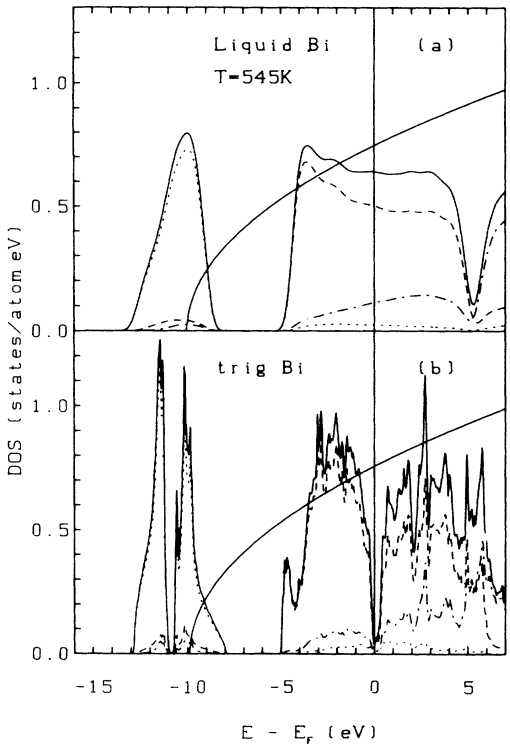

FIG. 8. Electronic density of states for liquid (a) and crystalline (b) Bi. For the key see Fig. 6.

The *s-p* gap is related on one hand to the relativistic lowering of the *s* level relative to the *p* level and on the other hand to structural effects. The *s-p* gap is structure induced; it is situated at an energy $E_B = (\hbar^2/2m)(Q_p/2)^2$ above the bottom of the band, where Q_p is the wave vector corresponding to the first peak in $S(q)$, the width of the gap scales with the amplitude $S(Q_p)$ multiplied with the pseudopotential matrix element $w(Q_p)$—both increase in the sequence As, Sb, and Bi. The increase in the matrix element $w(Q_p)$ has its origin in the relativistic effects and is related to a decrease in $w(2k_F)$ (with $2k_F \gg Q_p$) — which in turn causes the damping of the Friedel oscillations and the change in the structure. Hence the trends in the structure and in the electronic spectrum may be understood in a really consistent way, and for all polyvalent *s-p* bonded elements (cf. Ref. 1).

The DOS at the Fermi level is of the order of the free-electron DOS. Altogether, the DOS of the liquid elements is definitely metallic. This is correct for liquid Sb and Bi but incorrect for liquid As. For liquid As our results derived from the LMTO supercell calculations can be compared with the dynamical-simulated-annealing (DSA) results of Hafner and Payne[47] and the *ab initio* density-functional molecular dynamics of Li *et al.*[21] In contrast to the LMTO-ASA and DSA results based on pair forces, the DF-MD results show a pseudogap at the Fermi level. This demonstrates that the existence of the pseudogap depends very sensitively on four-body correlation functions—in this case on the correlation function measuring the average height of a distorted trigonal As_4 pyramid. This is the lowest level of many-body correlations at which a significant difference with the pair-potential simulation and the *ab initio* DF-MD simulation appears.

For liquid Sb and Bi the prediction of a metallic DOS at the Fermi level is in agreement with experiment, but a quantitative assessment requires a careful comparison with photoemission data.

B. Photoemission intensities

The photoemission intensities may be calculated as an average of the local, angular-momentum-decomposed DOS $n_l(E)$, weighted with the partial photoionization cross section $\sigma_l(E,\hbar\omega)$. The $\sigma_l(E,\hbar\omega)$ can be computed as a function of the binding energy E of the photoelectron and of the energy $\hbar\omega$ of the incident photon in a single-scatterer final-state approximation, and completely neglecting wave-vector conservation.[47–49] In the crystalline state, the last assumption is valid only for x-ray excitation (XPS) where phonon broadening relaxes the wave-vector conservation, in the liquid state it applies even to low excitation energies. For any details, we refer to Refs. 1 and 2.

Figure 9 shows the photoionization cross sections and the photoelectron intensities for crystalline Sb and Bi, calculated for Al $K\alpha$ excitation ($\hbar\omega$ = 1486.6 eV), and compared with the experimental data of Ley *et al.*[7,45] The calculated spectra have been convoluted with a Gaussian of width σ = 0.5 eV, to account for the limited experimental resolution. Agreement between theory and experiment is very good, except for the splitting of the *p* band in Bi, which is due to spin-orbit effects and is neglected in our scalar relativistic calculation.

Figure 10 shows the photoemission intensity of liquid Bi, calculated for different energies of the exciting pho-

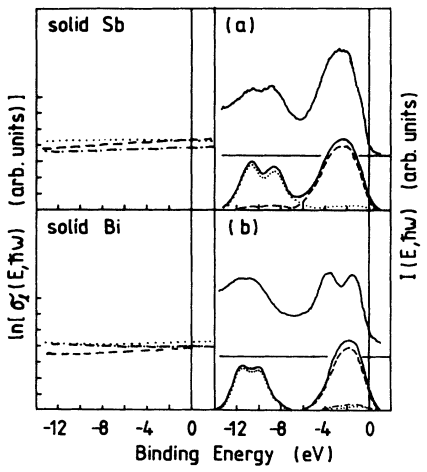

FIG. 9. Photoionization cross sections $\sigma_l(\hbar\omega, E)$ and photoemission intensities $I(E)$ for crystalline Sb (a) and Bi (b), calculated for Al-Kα excitation. For the key see Fig. 6. The experimental data are from Ley *et al.*, Refs. 7 and 45.

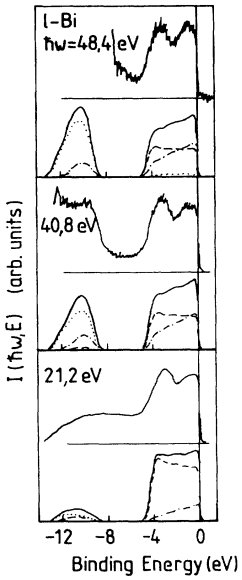

FIG. 10. Photoemission intensity $I(E)$ for liquid Bi, calculated for different photon energies. For the key see Fig. 6. The experimental data are from Oelhafen *et al.*, Ref. 16.

ton. We find that the cross section varies strongly with the photon-energy: at low excitation energies the spectrum is dominated by the p contribution. At higher photon energies the s and the p bands are about equally weighted, but the largest cross section is calculated for the d electrons. Except for the missing spin-orbit splitting we again find excellent agreement between theory and experiment.[16] In particular the complete splitting of the s and p bands and the metallic character of the DOS are confirmed by the experiment.

IV. TRENDS ACROSS THE PERIODIC TABLE AND CONCLUSIONS

We have extended our investigations of the structural and electronic properties of the liquid polyvalent elements to the semimetals As, Sb, and Bi. We find that the simple arguments for the existence of open, low-coordinated liquid structures in the light polyvalent elements, and the return to a more close-packed arrangement with increasing atomic number, also apply to the pentavalent elements. The return to a close-packed structure is related to the appearance of a structure-induced minimum in the DOS at an energy $(\hbar^2/2m)(Q_p/2)^2$ above the bottom of the valence band. This gap is related on the other hand to the relativistic s-p splitting, which determines the variation of the effective interatomic potential and in turn the liquid structure. Hence we now have a consistent picture of the trends in the structural and electronic properties of all s-p bonded elements from Li to Bi and Te.[27] These trends are summarized in Figs. 11 and 12. Even for the elements that remain semiconducting in the liquid state (As, Se, and Te at not too high temperatures), the pair and triplet correlations are well described in terms of volume and pair forces. The "anomalous" side peaks or shoulders to the first diffraction peak always occur very close to $q = 2k_F$ (Fig. 11). This indicates the importance of the Friedel oscillations for the liquid structures. In the semiconducting melts, many-body forces are important for $n \geq 4$ particle correlations. These correlations in turn are very important for the existence of the gap at the Fermi level.[21,27] The fact that the existence of the semiconductor gap depends on the correct description of higher-order correlation functions is by itself an important result for understanding the interrelation between changes in the atomic structure and the metal-nonmetal transition. This point certainly deserves further investigation.

Leaving the liquid semiconductors aside, we find that our calculations describe the trends in the electronic structure across the periodic table, from Li to Bi, very well (see Fig. 12). We predict two essentially different mechanisms that can cause deviations of the DOS from a free-electron parabola. (i) A structure-induced s-p gap is found in the elements where a strong first peak in the structure factor at $q = Q_p$ combines with a large electron-ion pseudopotential matrix element $w(Q_p)$. This is the case for the first-row elements Li and Be and for the heavy polyvalent elements (Hg, In, Tl, Ge, Sn, Pb, Sb, and Bi). (ii) For the heavy alkali- and alkaline-earth metals, the incipient occupation of the d states leads to a marked deviation from the free-electron DOS.

The calculations described in this series could, in principle, be done using *ab initio* density-functional molecular-dynamics calculations, without resorting to perturbation theory. So why is there still an interest in these simpler calculations? One point is, of course, that the perturbative approach is much faster. All the results summarized in Figs. 11 and 12 may be obtained in less computer time than is necessary for a DF-MD calculation for a single element. The older approach is predictive for all metallic elements where linear response theory applies. Even for the semiconducting liquids, where this no longer holds, the comparison of the pair-potential calculations with the DF-MD approach based on the full set of quantum-mechanical many-body forces is very instructive. This comparison elucidates the important role of the interplay of volume and pair forces. It demonstrates that attempts to model the interatomic force field in liquid metals and semiconductors using classical pair and triplet forces are bound to fail, if they do not account for the important effect of the volume forces. On the other hand, efficient techniques for atomistic simulations could be developed on the basis of a combination of the perturbative and the DF-MD approach.

Furthermore, not all the elements covered in this study can be treated using DF-MD. This applies to the IIb metals, where a narrow d band overlaps with the bottom of the s,p band and the heavy Ia and IIa elements, where the nearly empty d band overlaps with the conduction band. Also, the calculation of the partial photoionization cross sections, which is very important for the quantitative analysis of the photoemission intensities, requires the angular-momentum decomposition of the DOS, which can be obtained in the LMTO basis but

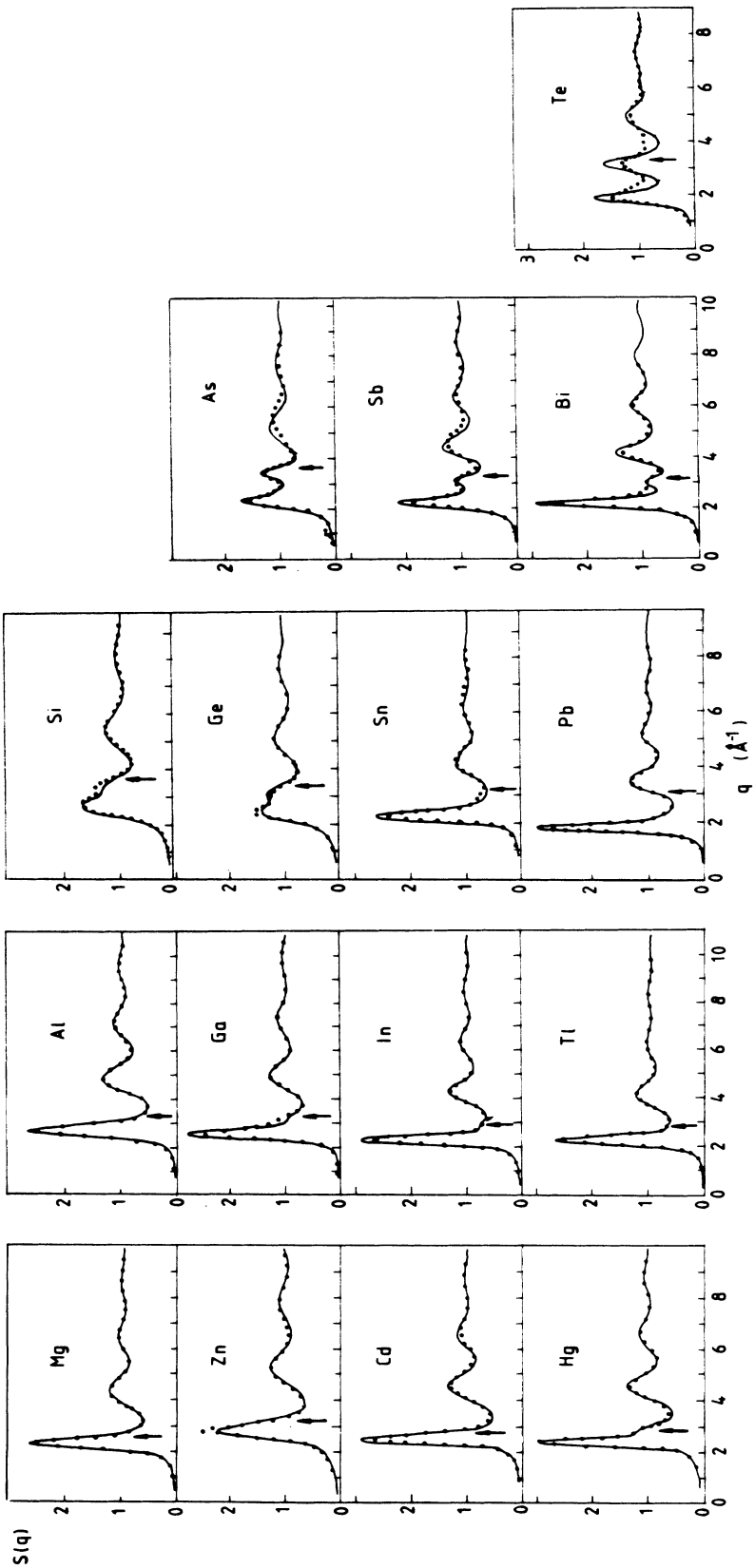

FIG. 11. Trend in the static structure factor $S(q)$ of the liquid metals across the periodic table. Full line—theory, dots—experiment. The vertical arrow indicates the wave vector $q = 2k_F$; see the text, Refs. 1, 2, and the present work.

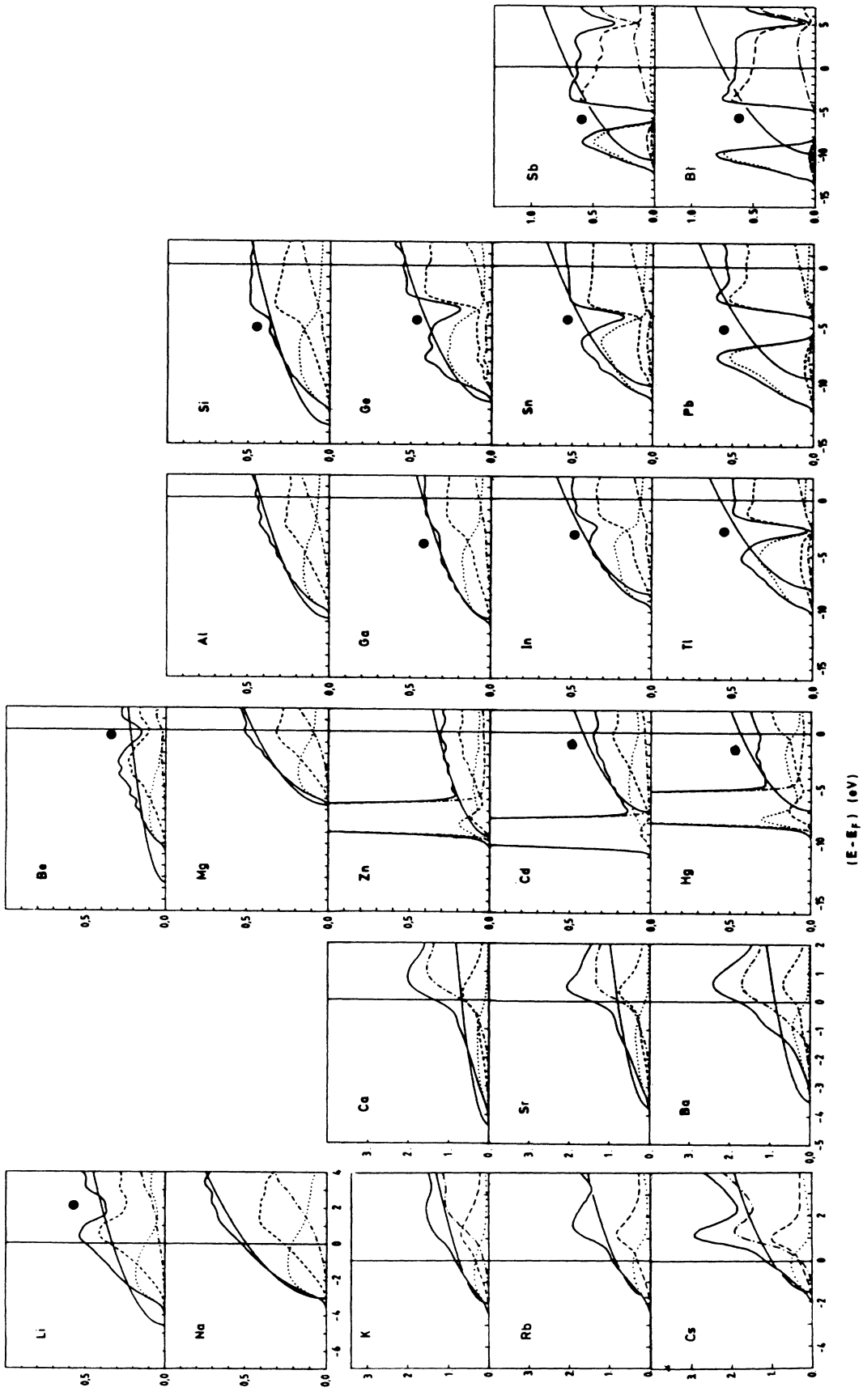

FIG. 12. Trend in the electronic DOS of the liquid metals across the periodic table. For the key see Fig. 6. The full dots mark the energy $(\hbar^2/2m)\,(Q_p/2)^2$, where Q_p is the wave vector of the first peak in the static structure factor $S(q)$. See the text, Refs. 1, 2, and the present work.

not with plane waves.

To conclude, we now have a complete picture of the trends in the atomic and electronic structures of the liquids s,p bonded across the periodic table. The calculations are based on interatomic forces derived by perturbation theory, but the comparison with DF-MD results for the most difficult cases (ℓ–Si, ℓ–As) allows us to conclude that they are predictive for all liquid metallic elements. Similar studies for the liquid $3d$ and $4d$ elements have been published elsewhere.[50,51]

ACKNOWLEDGMENTS

We thank Professor P. Weinberger and Dr. J. Redinger for the program used to calculate the photoionization cross sections. Our work was supported by the Fonds zur Förderung der wissenschaftlichen Forschung under Project No. 7192. The numerical calculations were performed on an IBM-3090-400VF at the Computer Center of the University of Vienna, supported by the IBM European Academic Supercomputer Initiative (EASI).

[1] W. Jank and J. Hafner, Phys. Rev. B **41**, 1497 (1990); (b) **42**, 6926 (1990); (c) J. Hafner and W. Jank, *ibid.* **42**, 11 530 (1990).
[2] W. Jank and J. Hafner, J. Phys. Condens. Matter **2**, 5065 (1990); **3**, 6947 (1991).
[3] D. Schiferl and C.S. Barrett, J. Appl. Crystallogr. **2**, 30 (1969).
[4] P.B. Littlewood, Crit. Rev. Solid State Sci. **11**, 283 (1983).
[5] P.B. Littlewood, J. Phys. C **13**, 4855 (1980); **13**, 4875 (1980).
[6] Y.L. Yarnell, J.L. Warren, R.G. Wenzel, and S.H. Koenig, IBM J. Res. Dev. **8**, 234 (1964).
[7] L. Ley, R.A. Pollak, S.P. Kowalczyk, F.R. McFeely, D.A. Shirley, Phys. Rev. B **38**, 641 (1973).
[8] R. Bellissent, C. Bergman, R. Ceolin, and J.P. Gaspard, Phys. Rev. Lett. **59**, 661 (1987).
[9] G.N. Greaves, S.R. Eliott, and E.A. Davies, Adv. Phys. **28**, 49 (1979).
[10] M. Shimoji, *Liquid Metals* (Academic, New York, 1977).
[11] P. Lamparter, W. Martin, S. Steeb, and W. Freyland, J. Non-Cryst. Solids **61+62**, 279 (1984).
[12] Y. Waseda, *The Structure of Non-Crystalline Materials: Liquids and Amorphous Solids* (McGraw-Hill, New York, 1980).
[13] U. Dahlborg and M. Davidovic, Phys. Chem. Liq. **15**, 243 (1986).
[14] M. Dzugutov and U. Dahlborg, Phys. Rev. A **40**, 4103 (1989).
[15] W. Knoll, P. Lamparter, and S. Steeb, Z. Naturforsch. **38a**, 395 (1982).
[16] P. Oelhafen, G. Indlekofer, and J.-J. Güntherodt, Z. Phys. Chem. **157**, 483 (1988).
[17] J.P. Gaspard, R. Bellissent, C. Bergman, C. Bichara, A. Pellegatti, and R. Ceolin, J. Non-Cryst. Solids **106**, 108 (1988).
[18] J. Hafner, Phys. Rev. Lett. **62**, 784 (1989).
[19] J. Hafner, J. Phys. Condens. Matter **2**, 1271 (1990).
[20] J. Hafner, in *Many-Atom Interactions in Solids,* edited by R. Nieminen, M. Manninen, and M. Puska (Springer, Berlin, 1990), p. 144.
[21] X.P. Li, P.B. Allen, R. Car, M. Parrinello, and J.Q. Broughton, Phys. Rev. B **41**, 3260 (1990).
[22] J. Robertson, J. Phys. C **8**, 3131 (1975).
[23] M.J. Kelly and D.W. Bullett, Solid State Commun. **18**, 593 (1976).
[24] L.F. Mattheiss, D.R. Hamann, and W. Weber, Phys. Rev. B **34**, 2190 (1986).
[25] R.J. Needs, R.M. Martin, and O.H. Nielsen, Phys. Rev. B **33**, 3778 (1986); **35**, 9851 (1987).
[26] T. Sasaki, K. Shindo, and K. Niizeki, Solid State Commun. **67**, 569 (1988).
[27] J. Hafner and M.C. Payne, J. Phys. Condens. Matter **2**, 221 (1990).
[28] J. Hafner and V. Heine, J. Phys. F **13**, 2479 (1983).
[29] J. Hafner and G. Kahl, J. Phys. F **14**, 2259 (1984).
[30] V. Heine and D. Weaire, in *Solid State Physics,* edited by H. Ehrenreich, F. Seitz, and D. Turnbull (Academic, New York 1970), Vol. 24, p. 247.
[31] J. Hafner, *From Hamiltonians to Phase Diagrams* (Springer, Berlin, 1987).
[32] N.W. Ashcroft, Phys. Lett. **23**, 48 (1966).
[33] S. Ichimaru and K. Utsumi, Phys. Rev. B **24**, 7385 (1981).
[34] W. A. Harrison, *Pseudopotentials in the Theory of Metals* (Benjamin, New York, 1966).
[35] G. D. Bachelet, D.R. Hamann, and M. Schlüter, Phys. Rev. B **26**, 4199 (1982).
[36] A.M. Rappe, K.M. Rabe, E. Kaxiras, and J.D. Joannopoulos, Phys. Rev. B **41**, 1227 (1990).
[37] N. Troullier and J.L. Martins, Phys. Rev. B **43**, 1993 (1991).
[38] J.T. Devreese and F. Brosens, in *Electronic Structure, Dynamics, and Quantum Structural Properties of Condensed Matter,* Vol. 121 of *NATO Advanced Study Institute, Series B,* edited by J.T. Devreese and P. Van Camp (Plenum, New York, 1985).
[39] G. Kresse, J. Hafner, and R.J. Needs (unpublished).
[40] L. Reatto, D. Levesque, and J.J. Weis, Phys. Rev. A **33**, 3451 (1986).
[41] M. Dzugutov, in *Static and Dynamics Properties of Liquids,* edited by M. Davidovic and A.K. Soper (Springer, Berlin, 1989), p. 185.
[42] M. Dzugutov, K.E. Larsson, and I. Ebbsjö, Phys. Rev. A **38**, 3609 (1988).
[43] O.K. Andersen, O. Jepsen and D. Glötzel, in *Highlights of Condensed Matter Theory,* edited by F. Bassani, F. Fumi, and M.P. Tosi (North-Holland, Amsterdam, 1985).
[44] H.L. Skriver, *The LMTO Method* (Springer, Berlin, 1984).
[45] L. Ley, M. Cardona, and R.A. Pollak, in *Photoemission in Solids II,* Vol. 27 of Topics in Applied Physics, edited by L. Ley and M. Caronda (Springer, Berlin, 1979), p. 106.
[46] G.N. Greaves and E.A. Davis, Philos. Mag. **29**, 1201 (1974).
[47] T. Jarlborg and P.O. Nilsson, J. Phys. C **12**, 265 (1979).
[48] H. Winter, P. Durham, and. G.M. Stocks, J. Phys. F **14**, 1047 (1984).
[49] J. Redinger, P. Marksteiner, and P. Weinberger, Z. Phys. B **63**, 321 (1986).
[50] Ch. Hausleitner, G. Kahl, and J. Hafner, J. Phys. Condens. Matter **3**, 1589 (1991).
[51] W. Jank, Ch. Hausleitner, and J. Hafner, J. Phys. Condens. Matter **3**, 4477 (1991).